

GAS DISCHARGE CAPACITY INTENSIFICATION OF ADSORBED NATURAL GAS RESERVOIRS

Luciano G. Lara

Petrobras S/A – ENGENHARIA/IEABAST/EAB/ENPRO, Rio de Janeiro, RJ, 20031-004, Brazil
lglara@petrobras.com.br

Paulo Couto

Federal University of Rio de Janeiro – Petroleum Engineering – DEI/POLI, Rio de Janeiro, RJ, 21941-972, Brazil
pcouto@petroleo.ufrj.br

Renato M. Cotta

Federal University of Rio de Janeiro – PEM/COPPE, Rio de Janeiro, RJ, 21941-972, Brazil
cotta@serv.com.ufrj.br

Dayse M. A. Sophia

Federal University of Rio de Janeiro – PEM/COPPE, Rio de Janeiro, RJ, 21941-972, Brazil
dayse.sophia@gmail.com

Abstract. The discharge capacity intensification of an adsorbed natural gas reservoir under a slow discharge process is discussed in this work. A theoretical two-dimensional transient model, developed by the authors, was used to analyse the influence of heat transfer parameters on the discharge capacity. This model is also able to analyse the influence of a thermal control device located axially at the centre of the reservoir. A heat pipe is considered as a thermal control devices (a heat pipe is a two-phase flow heat transfer device). The coupling of the one-dimensional transient heat pipe model and the two-dimensional transient model for natural gas slow discharge is presented and discussed. The following parameters are analysed: convection heat transfer at the reservoir external wall, effective thermal conductive of activated carbon bed, thermal capacity of the reservoir wall and discharge mass flow rate. Regarding the heat pipe, the temperature of the heat source at the heat pipe's evaporator is analysed. The results of the analyses are shown and then discussed.

Keywords. Natural Gas, Adsorption, Heat Pipe, and Gas Transportation.

1. Introduction

Adsorption is the gas molecules uptake process in an interfacial layer (usually a highly porous media), whether by capillary condensation or by Van der Waals forces (Gregg and Sing, 1982). This new technology has been considered for natural gas storage and transportation in the last 10 years (Brady *et al.*, 1996; Mota *et al.*, 1997; MacDonald and Quinn, 1998; Vasiliev *et al.*, 2000a and 2000b; Burchell and Rogers, 2000; Litzke and Wegryzn, 2001; Biloé *et al.*, 2001a,b and 2002) as an alternative to Compressed Natural Gas (CNG) and Liquefied Natural Gas (LNG). In the case of natural gas, the uptake process occurs at relatively low pressures, in the order of 35 to 50 atmospheres, which provides three main benefits: (1) compression costs reduction, (2) increased safety of the reservoir, and (3) design flexibility of the storage tanks. Despite of these benefits, the storage capacity of ANG reservoirs is lower than LNG and CNG, being of the order of 90 V/V (Brady *et al.*, 1996) up to 164 V/V (Inomata *et al.*, 2002). The U.S. Department of Energy storage target for ANG vessels was set at 150 V/V and it was later revised to 180 V/V. According to Biloé *et al.* (2002), the performance and viability of an ANG system depends closely on the micro-porous characteristics of the adsorbent as well as on the heat and mass transfer properties. The problems affecting ANG technology associated with the heat and mass transfer properties are described below.

The concentration of the adsorbed phase, say q , in a porous matrix follows closely a power law function of the pressure, P , and temperature, T , of the reservoir, and it increases with pressure and decreases with temperature. Usually, the concentration is expressed as a function only of pressure for a given temperature and it is known as *adsorption isotherms* [$q = f(P)_T$]. Therefore, affinity must exist between the adsorbent bed and the gas to be adsorbed so that adsorption will occur naturally with increasing pressure. For natural gas, activated carbon has been used as adsorbent beds.

However, the adsorption phenomenon is an exothermic process. During the charging process of an ANG reservoir, the pressure increase will cause the natural gas to adsorb in the activated carbon bed. The gas, in the gas phase, must release energy to change from gas to adsorbed phase. This energy release is quantified by the latent heat of adsorption (ΔH) and it causes a temperature increase in the adsorbent bed, which according to the adsorption isotherm, results in less stored methane capacity under dynamic conditions (see Fig. 1 – left). This process can be compared to a condensation process.

In the other hand, during discharge of an ANG reservoir, the pressure drop caused by the gas extraction, will cause the adsorbed phase to change to the gas phase. This phase change will require an amount of energy (ΔH), which will be

taken from the adsorbent bed. Therefore, the desorption process is endothermic, cooling down the adsorbent bed. This temperature drop will cause some amount of gas to be retained inside the reservoir at depletion pressure, reducing the delivered methane capacity (Fig. 1 – right).

The thermal effects depend closely on the heat transfer properties of the adsorbent bed as well as on the external heat exchange at the vessel wall (Mota *et al.*, 1997 and Vasiliev *et al.*, 2000a and 2000b). Also, the high packing densities required for adsorbent beds (MacDonald and Quinn, 1998) create mass transfer limitations that limit the delivered and stored gas capacities (Mota *et al.*, 1997 and Biloé *et al.*, 2002).

This work will focus on the thermal problems affecting the discharge process of ANG reservoirs. A two-dimensional transient model developed by the authors (Lara, 2005) was used to analyse the effects of heat transfer parameters variation on the discharge capacity of ANG reservoirs. This discharge model was coupled to a one-dimensional transient model for a heat pipe device located axially at the centreline of the cylindrical reservoir (Lara *et al.*, 2006) to investigate the effects of the adsorbent bed thermal control on the discharge capacity. The results of this analyses is presented here. The objective is to contribute on the development of a large-scale low-pressure natural gas storage system for transportation applications in Brazil.

2. Literature Review

Understanding the dynamic response of an ANG reservoir when subject to a fast charge and/or slow discharge processes is an essential requirement for the design of such systems. Several authors have carried out the simulation of the charge and discharge processes of ANG reservoirs in the last decade (Chang and Talu, 1996; Mota *et al.*, 1997; Vasiliev *et al.*, 2000a and 2000b; and Biloé *et al.*, 2001a and 2002).

Chang and Talu (1996) presented a one-dimensional transient analysis of the slow discharge of a cylindrical ANG vessel. The authors measured the temperature drop in a commercial ANG cylinder during realistic methane discharge conditions to calculate the performance loss of the system. The performance was determined by comparing the volumetric storage capacity of the cylinder under dynamic conditions with that under isothermal condition (ideal situation). Experimental data showed that a temperature drop as high as 37°C can occur in the ANG vessel at a high discharge rate, resulting in a performance loss of 25% when compared to the isothermal capacity. At moderate discharge rates, the performance loss was expected to be around 15% to 20%. The experimental data also suggested that changing the gas flow direction from axial to radial increases the energy transfer to the central region of the ANG vessel. The authors accomplished this by using a perforated tube inserted at the central line to collect the exiting gas. Simulations showed that, by changing the direction of the gas flow, the dynamic loss was reduced to 12%, if compared to a loss of 22% without the perforated tube under similar discharge conditions. These authors also showed that the thermal conductivity of the packed adsorbent bed is one of the major obstacles for the commercial utilization of the ANG technology. However, little information was given on their experimental parameters and conditions regarding the heat transfer on the external wall of the reservoir.

A two-dimensional transient theoretical analysis of the fast charge and slow discharge of an ANG cylinder was discussed by Mota *et al.* (1997). The authors gave emphasis to thermal and mass diffusion effects in the activated carbon bed, and a complete mass, energy and momentum analysis was presented. Natural gas was modelled as ideal gas pure methane. Results for the fast charge simulation were in agreement with experimental results, and showed that a temperature rise as high as 79°C can occur in an ANG vessel. If there were no adsorption, the temperature rise would be only 7,7°C. Mass diffusion effects were included in the fast charge simulation causing a less pronounced temperature rise in the activated carbon bed. This is because intraparticle diffusional resistance reduces the momentum of the gas flowing in the cylinder, which causes a slower heat up rate of the system. Therefore, the storage system has more time to smooth the temperature rise by conduction. Slow discharge simulations showed that a temperature drop of 55°C can occur at the centre of the cylinder. The temperature drop at the cylinder external wall was 30°C. To increase the discharge performance of the ANG system the authors suggests: (1) increase the thermal conductivity of the bed by mixing

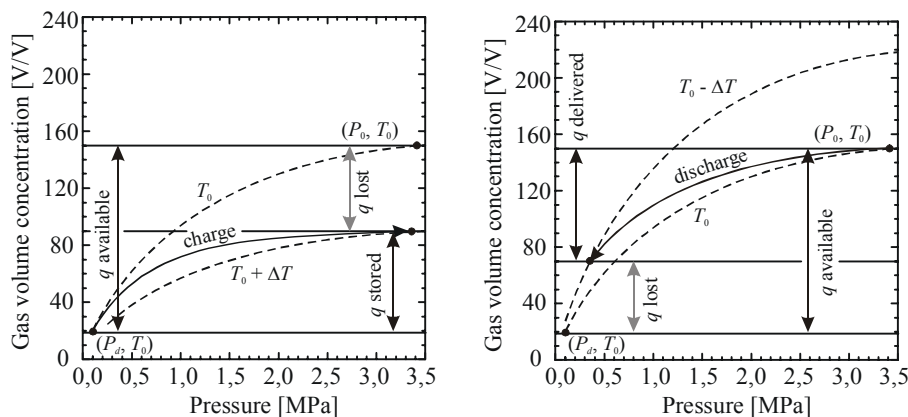


Figure 1. Charge (left) and discharge (right) processes of an ANG system.

the carbon particles, or replacing part of the binder in the case of carbon monoliths, with high conductivity material, (2) maintain the reservoir external wall at the highest possible temperature, in order to maximize temperature gradients in the bed and increase the heat transfer by conduction to the activated carbon bed, and (3) increase the external wall area per unit reservoir volume to increase heat transfer rate from the surroundings. However, none of these suggestions were investigated by the authors.

An experimental and theoretical investigation on ANG vessels was presented by Vasiliev *et al.* (2000a and 2000b). The authors proposed the use of heat pipes to increase the temperature of the activated carbon bed during methane discharge, and therefore, increase the amount of gas delivered. A temperature drop of about 25°C was experimented during discharge. A new type of activated carbon structure (Busofit AYTМ-055) was used in the experimental work, showing a storage capacity of 150 V/V. Although suggesting the use of heat pipes, the authors did not modelled the heat pipe. The effects of the heat pipe were included as a prescribed heat flux boundary condition at the centre of the reservoir.

Biloé *et al.* (2001a) described the experimental and theoretical evaluation of an ANG system using a new highly conductive adsorbent matrix. The adsorbent composite block was a mixture of super-activated carbon and expanded natural graphite, followed by consolidation. The thermal conductivity obtained for the new adsorbent matrix was 30 times higher than that of regular activated carbon bed. In their experimental work, Biloé and collaborators (2001a) considered that the external wall heat transfer is driven by forced convection of water and air. Experimental data agreed very well with theoretical data obtained from the solution of their one-dimensional transient model. At the centre of the vessel, a temperature drop of 5°C was experimented with the water forced convection experimental condition, and 40°C with the air forced convection experimental condition. The wall temperature drop was 1,5° and 37°C respectively, showing that the temperature gradients within the new highly conductive adsorbent matrix were very small, for both experimental conditions. The delivered methane capacity was close to 94 V/V and 71 V/V for the water forced convection situation and air forced con-vection situations, respectively.

Later, Biloé *et al.* (2002) presented a methodology for the optimization of ANG systems based on the Dubinin-Astakhov adsorption equilibrium relation. The heat and mass transfer limitations were implicitly introduced in the Dubinin-Astakhov equation by means of temperature and pressure drops. The authors stated that, based on the Dubinin relation “*the activated carbon must have a highly porous potential, a very narrow microporosity, and an average micropore width of 1,5 nm and 2,5 nm for the charge and the discharge step, respectively*”.

Although the literature presents suggestions to improve the storage capacity of ANG systems, the thermal control of this system was barely studied. This work will now address the modelling of an ANG reservoir considering a thermal control to overcome the adverse effects of the temperature gradient in order to enhance the natural gas storage capacity.

3. Theoretical Analysis

The natural gas admission in a power cycle is controlled by power requirements of the system. In this case, discharge time is increased considerably by the slow rate of natural gas discharge, which usually occurs at a constant flow rate outward the cylinder at the opening (Mota *et al.*, 1997). The heat of adsorption during this process decreases the temperature of the adsorbent bed, which in turns, increases the amount of natural gas retained inside the cylinder at depletion (Biloé *et al.*, 2002). However, the discharge process is not adiabatic, and the heat transferred from the surroundings to the cylinder partially compensates this “cooling” effect.

A model to predict the thermal behaviour of an ANG reservoir during the slow discharge process was developed by Lara (2005). This model considers the energy and a mass conservation equation. The energy equation accounts for the contribution of the solid phase (adsorbent), gas phase (adsorbate), and the adsorbed phase in the total energy stored in the reservoir. Also, the contribution of the energy transfer by heat diffusion in the solid phase is considered. The latent heat of adsorption is considered as a rate of internal heat generation. The assumptions made are: (1) instantaneous phase equilibrium between the adsorbed phase and the gas phase within the porous structure, (2) the local temperature of the adsorbent and free gas volume is the same due to a high intensity heat transfer between solid and gas phases (Bejan, 1995). Also, (3) for the solid and adsorbed phases, the internal energy depends only on the local thermodynamic temperature (Moran and Shapiro, 2000) and (4) the adsorbed phase is considered incompressible (Tien, 1994). As the discharge process is considered to be slow, (5) the pressure gradient inside the cylinder is negligible (Mota *et al.*, 1997), *i.e.*, the pressure is a function of time, only. So, the energy equation is written as:

$$(\varphi_{eff}c_{p,g}\rho_g + \rho_s c_{p,s} + \rho_s c_{p,g}q) \frac{\partial T}{\partial t} = \nabla \cdot (k_{eff} \nabla T) + \left[\varphi_{eff} \frac{dP}{dt} - \rho_s \Delta H \frac{\partial q}{\partial t} \right] \quad (1)$$

The boundary conditions of Eq. (1) are:

$$k_{eff} \nabla T \cdot \mathbf{n} + \rho_w c_{p,w} \delta_w \frac{\partial T}{\partial t} = h_\infty (T_\infty - T) \text{ for } \begin{cases} x = 0; & R_0 < r \leq R_{ext} \\ x = L; & 0 \leq r \leq R_{ext} \\ r = R_{ext}; & 0 \leq x \leq L \end{cases} \quad (2)$$

$$\nabla T \cdot \mathbf{n} = 0 \text{ for } \begin{cases} x = 0; & 0 \leq r \leq R_0 \\ r = 0; & 0 \leq x < L \end{cases} \quad (3)$$

Boundary conditions (2) accounts for the thermal capacity of the cylinder wall ($\rho_w c_{p,w}$) and for the heat transfer by natural convection, h_{ex} , at the external wall of the cylinder. A 2nd type boundary condition (3) is considered at the gas discharge region ($0 \leq r \leq R_0$) because the gas is assumed to leave the cylinder with the same local temperature of the system. The heat transfer coefficient can be obtained from natural convection correlations for horizontal cylinders (Bejan, 1995). The mass conservation equation considered in this model is:

$$\dot{m} = 2\pi \frac{d}{dt} \int_0^L \int_0^{R_{ext}} (\rho_{eff} \rho_g + \rho_s q) r dr dx \quad (4)$$

The two terms inside the integral expression represents the contribution of the gas and adsorbed phases in the total gas mass inside the cylinder. The time variation of the total gas mass inside the cylinder must be equal the mass flow rate outward the reservoir.

This model considers a Langmuir equilibrium relation (adsorption isotherm) for the adsorption of methane in an activated carbon bed, as given by Mota *et al.* (1997):

$$q = (q_m bP)/(1 + bP) \quad (5)$$

$$q_m = 55920T^{-2.3}, \quad \text{and} \quad b = 1.0863 \times 10^{-7} \exp(806/T)$$

Natural gas is modelled as pure methane, whose thermodynamic behaviour is modelled as ideal gas

3.1. Heat Pipe Device Model

A Heat Pipe is considered as a thermal control device for the ANG reservoir. Heat pipes are highly reliable and efficient heat transfer devices considered for many terrestrial and space applications (Peterson, 1991). This device uses the latent heat of vaporization (condensation and evaporation) of a working fluid to transfer relatively large amounts of energy over a long distance with a small temperature drop. Usually, heat pipes are composed of a sealed container with a wick structure adjacent to the inner wall, and it is divided into three regions: evaporator section, adiabatic (transport) section, and condenser section. The container of the heat pipe is evacuated and filled with a working fluid. During normal operation, the working fluid remains in a saturation condition, with liquid trapped in the wick structure and vapour in the core section, named vapour region. The heat flux applied to the evaporator section is conducted through the container wall and wick structure vaporizing the saturated liquid, increasing the local vapour pressure. The vapour resulting from the evaporation process flows through the adiabatic section towards the condenser end, where it condenses into the wick structure, releasing its latent heat of vaporization to a heat sink. The capillary forces developed in the wick structure pumps the working fluid back to the evaporator section. This process continues as long as there is sufficient capillary pressure to drive liquid back to the evaporator (Faghri, 1995). The heat pipe is modelled as a one-dimensional rod with length L_{HP} , radius R_{HP} , and a high conductivity k_{HP} , which can be determined from experimental results for temperature drop versus heat load (*e.g.*, Faghri, 1995). Thus, the energy balance for the heat pipe is given by:

$$(\rho c_p)_{HP} \frac{\partial T_{HP}}{\partial t} = k_{HP} \frac{\partial^2 T_{HP}}{\partial x^2} + \frac{2}{R_{HP}} k_{eff} \frac{\partial T}{\partial r} \Big|_{r=R_{HP}^*}; \text{ for } (L - L_{HP}) < x < L \text{ and } r = 0 \quad (6)$$

In equation (6), the term on the left hand side accounts for the thermal capacity of the heat pipe. The first term on the right hand side accounts for the axial heat diffusion over the heat pipe length while the last term couples the heat pipe energy equation with the adsorbent bed. It is important to observe that, in the last term on the right hand side of equation (6), the temperature gradient is calculated in the adsorbent bed and not on the heat pipe. Equation (6) is valid from $x = L - L_{HP}$ to $x = L$. The boundary condition for T_{HP} at $x = (L - L_{HP})$ required for equation (6) is given by:

$$k_{HP} \nabla T_{HP} \cdot \mathbf{n} = k_{eff} \nabla T \cdot \mathbf{n} \quad (7)$$

The boundary condition at $x = L$ is obtained from an energy balance at the evaporator region of the heat pipe. It is considered that heat is supplied at the evaporator section by forced convection of a hot fluid (*e.g.*, exhaust gas from internal combustion engines, wasted water vapour, etc.) with temperature T_f :

$$k_{HP} \frac{\partial T_{HP}}{\partial x} \Big|_{x=L} = (\rho c_p)_{HP} L_{evap} \frac{\partial T_{HP}}{\partial t} \Big|_{x=L} + \frac{2L_{evap}}{R_{HP}} h_f (T_{HP} - T_f) \quad (8)$$

where T_{HP} is the one-dimensional temperature distribution of the heat pipe, L_{evap} is the evaporator length, h_f is the heat transfer coefficient on the evaporator external wall, and T_f is the temperature of the heat source I this region. Correlations for forced convection over horizontal cylinders are considered for the calculation of h_f .

To couple the one-dimensional heat pipe model and the ANG discharge model of Lara (2005), a boundary condition at $r = 0$ and $(L - L_{HP}) < x < L$ of the later model must be set. Temperature continuity between the heat pipe and the adsorbent bed is considered as the boundary condition for this region.

4. Discharge Capacity Intensification Analysis

The parameters considered for the analyses presented in this work are shown in Table 1. These parameters are the same as those used for Mota *et al.*, 1997. Two mass flow rates are considered for each parameter analysis: $\dot{m} = 0.1641$ g/s and $\dot{m} = 0.3283$ g/s. These mass flow rates were obtained from the work of Mota *et al.* (1997). A performance coefficient is used to compare the results for each analysis. This coefficient compares the real gas mass delivered with the ideal (isothermal) gas mass delivered, and it is given by:

$$\eta = \frac{m_{delivered,real}}{m_{delivered,ideal}} = \frac{m_{delivered,real}}{\{[\varphi_{eff} \rho_g(T_0, P_0) + \rho_s q(T_0, P_0)] - [\varphi_{eff} \rho_g(T_0, P_f) + \rho_s q(T_0, P_f)]\} V_{cylinder}} \quad (9)$$

4.1 Effects of the Thermal Control Device

One way to overcome the adverse temperature gradient problem inside the activated carbon bed is to supply heat to the central region of the vessel using heat pipes. A water/stainless steel heat pipe is considered for the thermal control of the reservoir. Theoretical results for the temperature distribution within the adsorbent bed, discharged mass of gas, and performance coefficient η are presented for different T_f . The results are compared with the situation of no thermal control on the reservoir (Mota *et al.*, 1997). The heat transfer coefficient between the hot fluid and the evaporator section considered in this analysis is $h_f = 3000$ W/m²K, which is within the typical range for forced convection (Moran and Shapiro, 2000). Figures 2 and 3 show the temperature distribution within the adsorbent for the two mass flow rates considered at the end of the discharge process, *i.e.*, at depletion pressure. The leftmost plot on each figure represents the theoretical case analysed by Mota *et al.* (1997). It can be observed that the heat pipe is able to warm up the centre of the reservoir, but due to the poor thermal conductivity of the adsorbent bed the heating effect did not affected the entire adsorbent bed. Also, it can be observed that, for a slower discharge, *i.e.*, $\dot{m} = 0.1641$ g/s, the temperature gradients are slightly lower than for $\dot{m} = 0.3283$ g/s. This is because the heat diffusion has more time to spread its effects on the adsorbent bed, slightly increasing the average temperature, and thus, increasing the amount of gas discharged from the reservoir. Table 2 summarizes the results of this analysis.

Table 1. Parameters used for the discharge intensification analysis.

<i>Activated carbon bed properties:</i>		
Density – ρ_s	410	kg/m ³
Specific heat – $c_{p,s}$	650	J/kg.K
Effective conductivity – k_{eff}	1,2	W/m.K
Effective porosity – φ_{eff}	0,74	
<i>Cylinder geometry:</i>		
Material	Stainless steel	
Density – ρ_w	7900	kg/m ³
Specific heat – $c_{p,w}$	496,2	J/kg.K
External radius – R_{ext}	0,14	m
Length – L	0,85	m
Inlet radius – R_0	0,005	m
Thickness – δ_w	0,01	m
<i>Operational conditions:</i>		
Initial pressure – P_0	3,5	MPa
Depletion pressure – P_d	101,325	kPa
Initial temperature – T_0	285	K
Ambient temperature – T_∞	285	K
<i>Adsorption characteristics:</i>		
Heat of adsorption – ΔH	$-1,1 \times 10^6$ J/kg	
<i>Heat Pipe Dimensions:</i>		
Length – L_{HP}	0,8	m
Radius – R_{HP}	0,009525	m
Conductivity – k_{HP}	1500	W/m.K
Thermal capacity – $(\rho c_p)_{HP}$	$4,1 \times 10^6$ J/ m ³ .K	
Evaporator length – L_{evap}	0,2	m

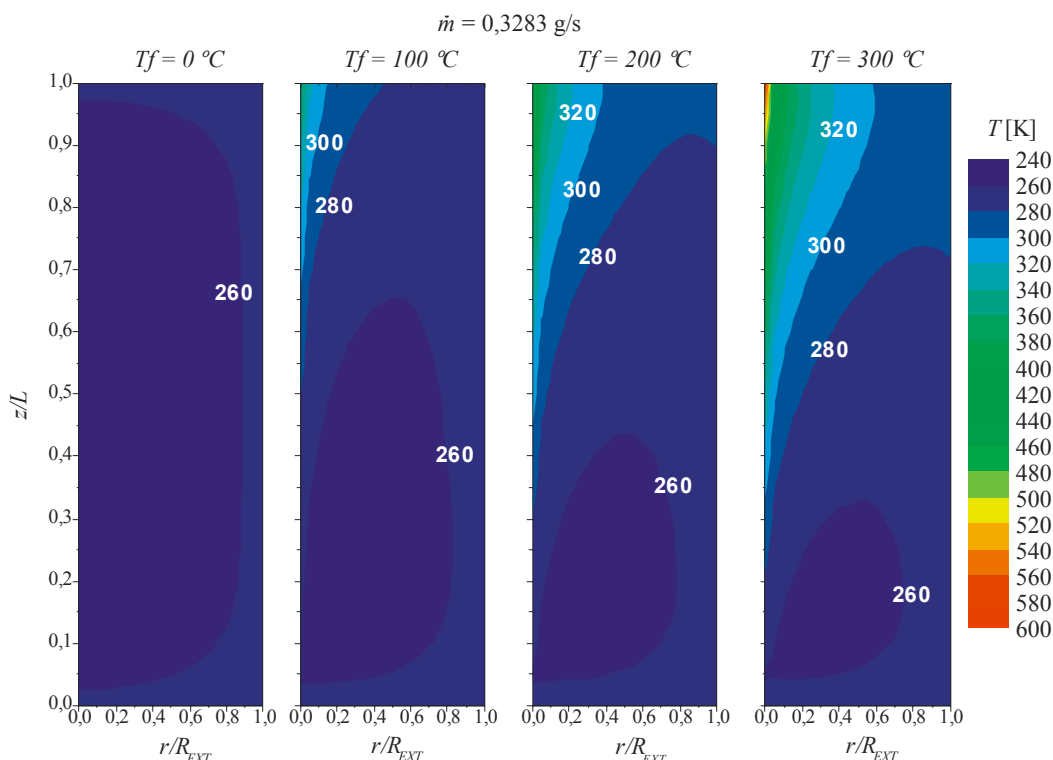


Figure 2: Temperature distribution within the adsorbent bed for $\dot{m} = 0,3283$ g/s at depletion pressure.

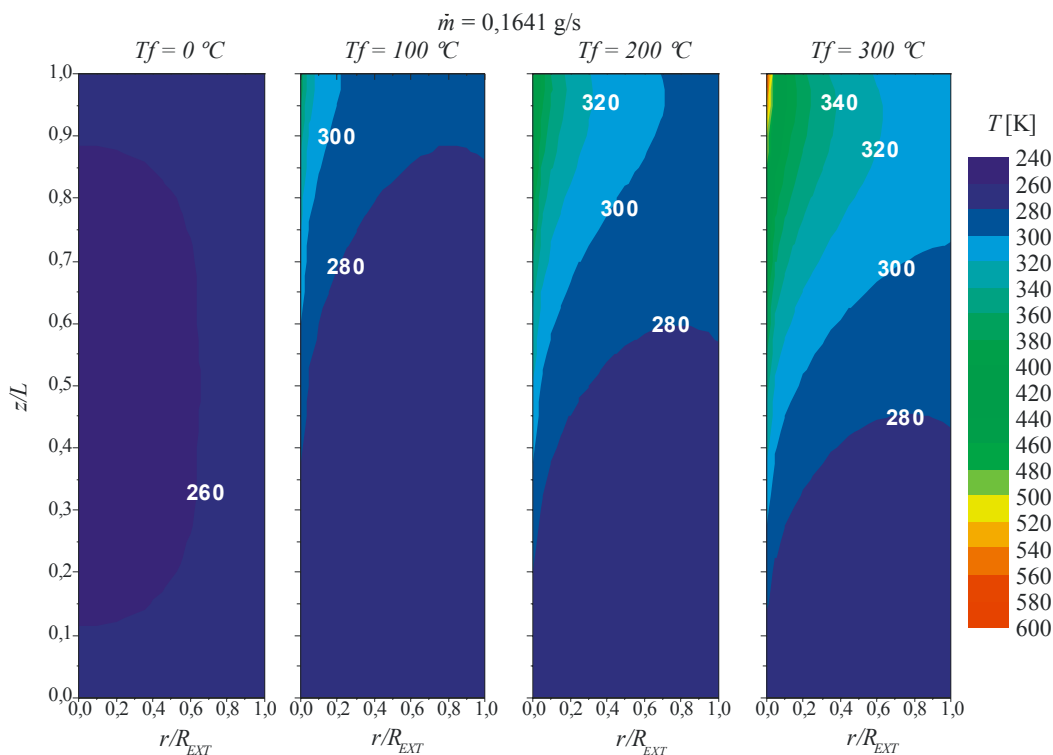


Figure 3: Temperature distribution within the adsorbent bed for $\dot{m} = 0,1641$ g/s at depletion pressure.

From Table 2, it is clear that the use of heat pipes in adsorbed natural gas reservoir is effective on increasing the discharge duration for a constant mass flow rate required by a power system, thus increasing the life-time of the refueling system. For the 50 litres cylinder considered here, and for $\dot{m} = 0,3283$ g/s, the performance coefficient increased from 88,02% for the case of no thermal control to 94,74% for the case of thermal control by heat pipe using a 300°C hot fluid as a heat source, which corresponds to an increase of 7,5% of the discharged mass of fuel. For $\dot{m} = 0,1641$ g/s, the increase of the discharged fuel mass was 8,8%.

Table 2: Results for the heat pipe analysis.

Mass flow rate [g/s]	T_f [°C]	Discharged mass (isothermal) [kg]	Discharged mass [kg]	η [%]	Discharge duration [h]
$\dot{m} = 0,3283$ g/s	No thermal ctrl.	2,687	2,367	88,02	2:00
	$T_f = 100$ °C	2,688	2,443	90,86	2:06
	$T_f = 200$ °C	2,688	2,498	92,94	2:11
	$T_f = 300$ °C	2,689	2,547	94,72	2:16
$\dot{m} = 0,1641$ g/s	No thermal ctrl.	2,688	2,442	90,84	4:13
	$T_f = 100$ °C	2,688	2,532	94,21	4:29
	$T_f = 200$ °C	2,688	2,601	96,75	4:40
	$T_f = 300$ °C	2,692	2,659	98,79	4:50

4.2. Effects of Convection Heat Transfer at Cylinder Wall

Another way to overcome the adverse temperature gradient inside the adsorbent bed is to increase the heat transfer between the cylinder wall and the surroundings to compensate for the reservoir cooling. For this analysis three surrounding temperatures (19°C, 100°C, and 200°C) and four different heat transfer coefficient between the cylinder and the surrounding [0 W/m².K, 4,5 W/m².K (natural convection), 15 W/m².K, 1000 W/m².K] are considered. The $h_w = 0$ W/m².K situation correspond to a thermally insulated cylinder. For natural convection, the coefficient is obtained from well known correlations available in the literature (Bejan, 1995). Higher surrounding temperatures can be obtained by circulating a high temperature gases around the reservoir (Mota *et al.*, 2004). Figures 4 and 5 show the temperature distribution on the adsorbent bed for $T_\infty = 19$ °C and $\dot{m} = 0,3283$ g/s, and for $T_\infty = 200$ °C and $\dot{m} = 0,1641$ g/s, respectively. Table 3 summarizes the results for this analysis. The complete set of results can be found in Lara (2005).

It is interesting to observe that for higher surrounding temperatures and higher heat transfer coefficient, the performance coefficient η is above 100%. This is because the heat transfer intensification due to the higher convection coefficient and to the higher surrounding temperature increases the activated carbon bed temperature above the isothermal limit. The bed temperature increase causes an increase in the reservoir pressure maintaining constant the mass flow rate at the reservoir opening. This pressure increase can extend the discharge duration in up to 35 minutes. It can be seen that the convection heat transfer plays an important role in the discharge duration, but the most important parameter is the surrounding temperature, T_∞ . For the same heat transfer coefficient, the increase in T_∞ from 19 °C to 100 °C can extend the discharge duration in up to 20 minutes.

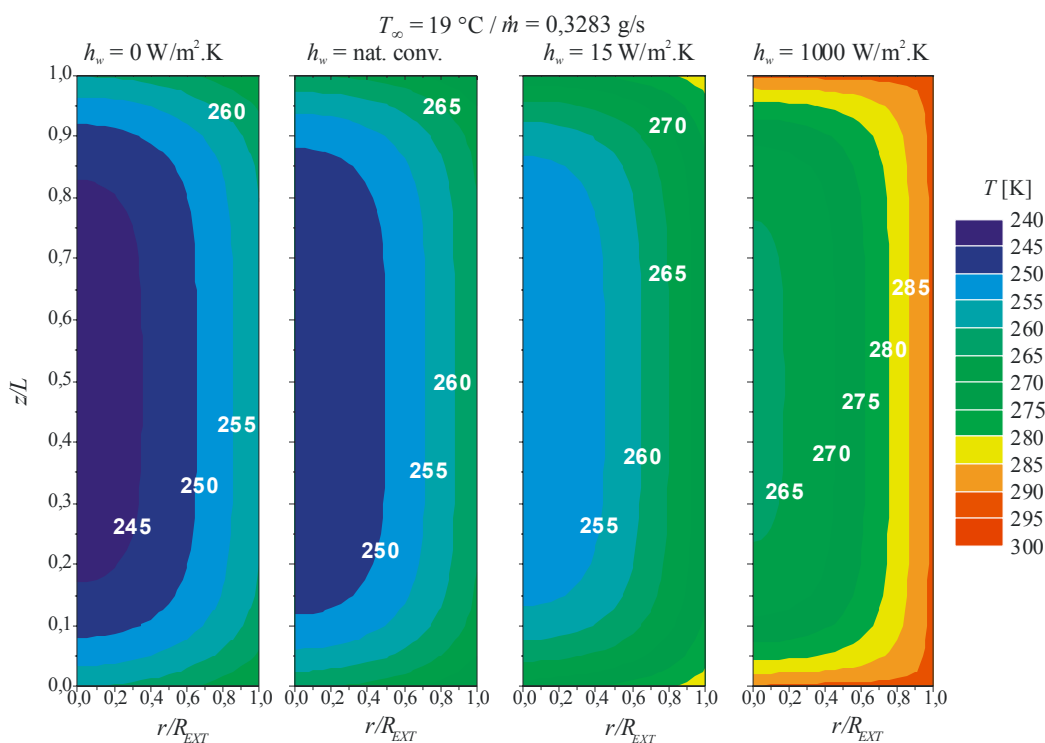


Figure 4: Temperature distribution within the adsorbent bed for $T_\infty = 19$ °C and $\dot{m} = 0,3283$ g/s at depletion pressure.

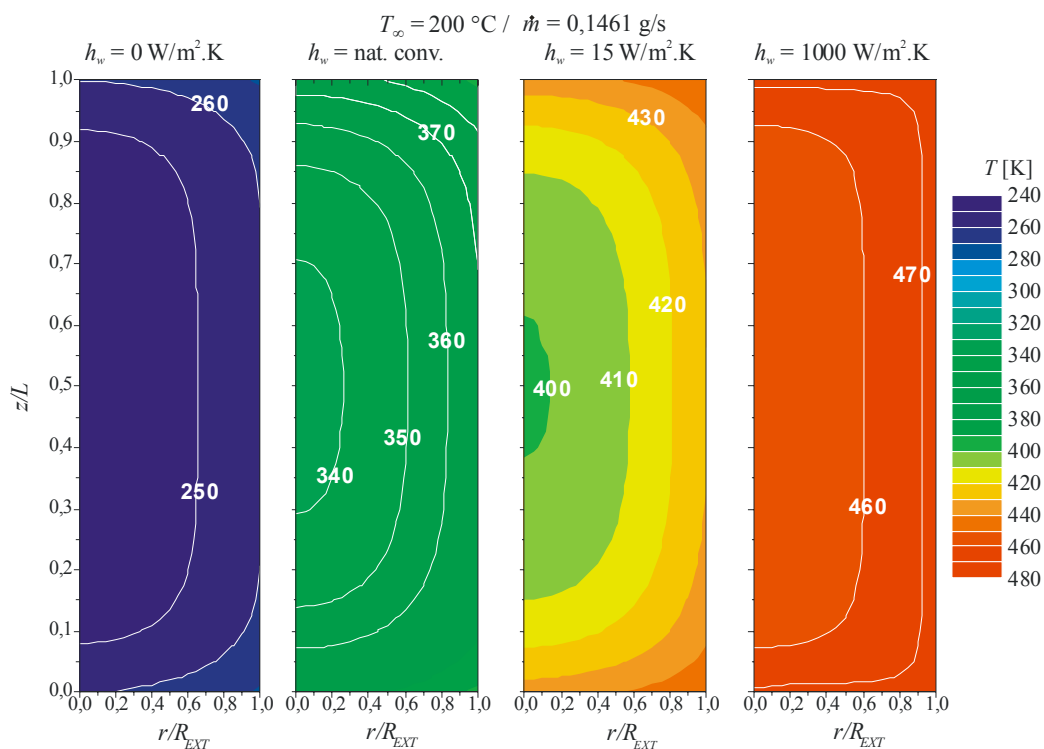


Figure 5: Temperature distribution within the adsorbent bed for $T_\infty = 200\text{ °C}$ and $\dot{m} = 0,1461\text{ g/s}$ at depletion pressure.

Table 3. Results for the heat transfer coefficient and surround temperature analysis.

h_w [W/m ² K]	Discharged mass [kg]	η [%]	Discharge duration [h]
$T_\infty = 19\text{ °C}$			
0	2,318	86,21	1:57
Nat. conv.	2,367	88,02	2:00
15	2,453	91,23	2:04
1000	2,600	96,71	2:12
$T_\infty = 100\text{ °C}$			
0	2,318	86,21	1:57
Nat. conv.	2,708	100,71	2:17
15	2,856	106,23	2:25
1000	2,929	108,86	2:28
$T_\infty = 200\text{ °C}$			
0	2,318	86,21	1:57
Nat. conv.	2,922	108,80	2:28
15	2,998	111,57	2:32
1000	3,024	112,61	2:33

Figure 6 shows the influence of the surrounding temperature, T_∞ , on the pressure profiles as a function of the discharge time for the four h_w cases studied in this work. This influence increases considerably for the pressure profiles for $h_w = 1000\text{ W/m}^2\text{K}$ and $T_\infty = 100\text{ °C}$ (Fig. 6 - left) and for $h_w = 1000\text{ W/m}^2\text{K}$ and $T_\infty = 200\text{ °C}$ (Fig. 6 - right). Observing the simulation for $T_\infty = 100\text{ °C}$ and $h_w = 1000\text{ W/m}^2\text{K}$, from the beginning of process to almost 15 minutes of discharge time, the effects of the heat transferred by convection to the cylinder is predominant comparing to the latent heat of adsorption cooling effects, causing the pressure to increase. After this point, the latent heat of adsorption cooling effects overcomes the convection heat transfer, and the gas pressure begins to decrease as mass is removed from the reservoir.

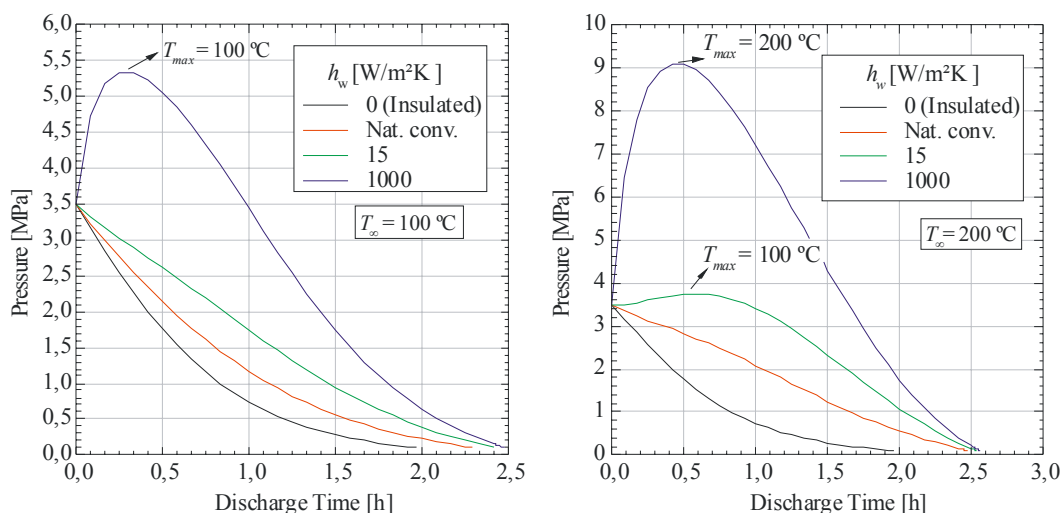


Figure 6: Effects of h_w on the gas pressure inside the reservoir for $T_\infty = 100\text{ }^\circ\text{C}$ (left) and $T_\infty = 200\text{ }^\circ\text{C}$ (right).

If the pressure increase provides longer discharge durations, in the other hand, it goes against the advantage of a low pressure reservoir as in the case of $T_\infty = 200\text{ }^\circ\text{C}$ and $h_w = 1000\text{ W/m}^2\cdot\text{K}$ when a maximum gas pressure of 9,2 MPa was observed inside the cylinder. At that point, the bed temperature adjacent to the wall cylinder achieved almost the same value of the surrounding temperature. However, from Table 3, the increase in the discharge duration time for h_w increasing from 15 $\text{W/m}^2\cdot\text{K}$ to 1000 $\text{W/m}^2\cdot\text{K}$ is not so large to compensate for an excessive gas pressure in the reservoir. The conclusion is that the heat transfer to the cylinder must be done in a controlled way to prevent high gas pressure inside the cylinder.

4.3. Effects of Effective Thermal Conductive of Carbon Bed

The analysis of the effects of the activated carbon bed thermal conductive was conducted considering four values of k_{eff} for different materials available in the literature (Chang and Talu, 1996; Mota *et al.*, 1997; and Biloé *et al.*, 2001b), with surrounding temperature of 19 °C, h_w given by natural convection, and mass flow rate of 0,3283 g/s. These parameters are presented in Tab. 4. The k_{eff} effects on the bed temperature at depletion pressure are shown in Fig. 7. It is clear that the higher the effective thermal conductivity, the smother is the temperature gradient in the activated carbon bed. Table 5 shows the k_{eff} effects on the system's performance coefficient. There is an evolution between the first three groups of carbon. The C3 activated carbon presented a performance equivalent to the C2. In fact, both materials were tested by Biloé *et al.* (2001b), presenting similar experimental results.

Table 4: Thermophysical properties values for activated carbon bed.

Parameter	Chang & Talu (1996)	Mota <i>et al.</i> (1997)	Biloé <i>et al.</i> (2001b)	Biloé <i>et al.</i> (2001b)
Material type	N/A	G216 carbon pellets	C2 ^(*)	C3 ^(*)
k_{eff} [W/m.K]	0,212	1,2	4,4	7,3
ρ_s [kg/m ³]	487,5	410	432	475
c_{ps} [J/kg.K]	1052	650	650 ^(**)	650 ^(**)

^(*) Matrix made of Expanded Natural Graphite ENG and Superactivated Carbon (Maxsorb).

^(**) Value inferred from performance coefficient data provided by Mota *et al.* (1997).

Table 5: Results for the effective thermal conductivity analysis.

k_{eff} [W/m.K]	Discharged Mass [kg]	η [%]	Discharge Time [h]
0,212	2,183	81,23	1,85
1,2	2,367	88,02	2,00
4,4	2,420	90,00	2,05
7,3	2,429	90,34	2,06

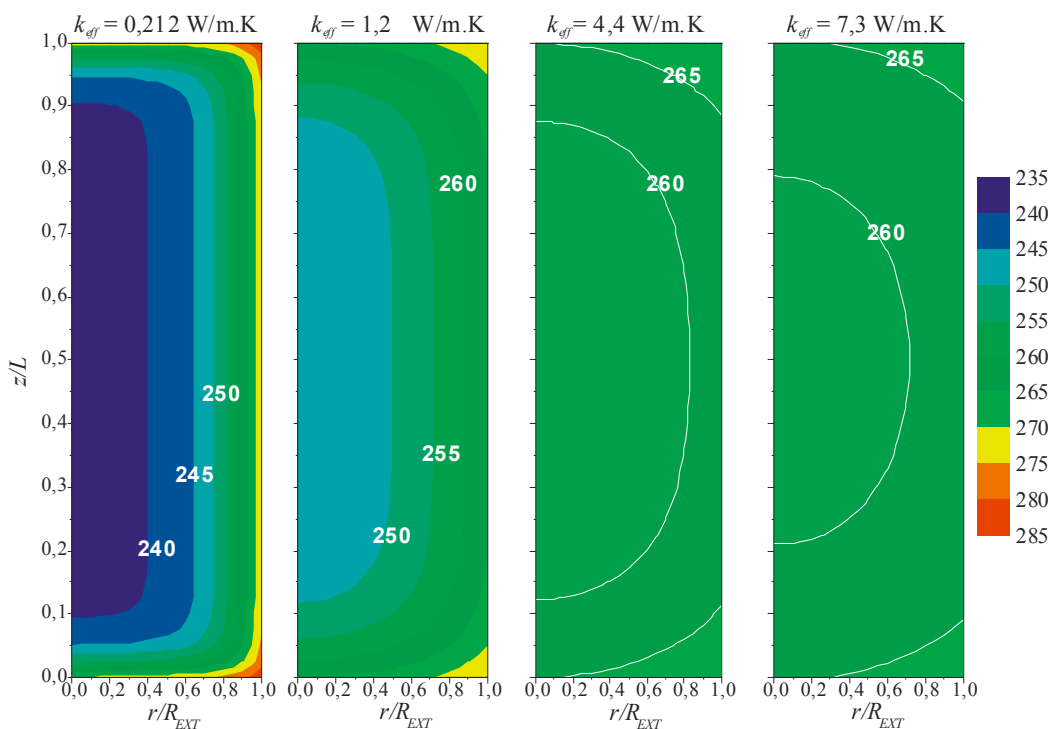


Figure 7: Temperature distribution within the adsorbent bed for $T_\infty = 19\text{ }^\circ\text{C}$ and $\dot{m} = 0,3283\text{ g/s}$ at depletion pressure.

4.4. Influence of Thermal Capacity of Cylinder Wall

This property is defined by $C_w = \rho_w c_{p,w} [\text{J/m}^3\cdot\text{K}]$, where ρ_w and $c_{p,w}$ are the density and specific heat of the cylinder wall. The following values for C_w were considered for analysis: $0\text{ J/m}^3\cdot\text{K}$, $1,96 \times 10^6\text{ J/m}^3\cdot\text{K}$ and $C_w = 3,92 \times 10^6\text{ J/m}^3\cdot\text{K}$. The last value was obtained from the work of Mota *et al.* (1997) and corresponds to a carbon steel cylinder. The analysis was performed for $T_\infty = 19\text{ }^\circ\text{C}$, $h_w = 4,5\text{ W/m}^2\cdot\text{K}$, $k_{eff} = 1,2\text{ W/m}\cdot\text{K}$, and $\dot{m} = 0,3283\text{ g/s}$, which correspond to the conditions experimented by Mota *et al.*, 1997. Figure 8 shows the temperature profile at depletion pressure, and Table 6 summarizes the results for the current analysis. It can be observed that higher cylinder wall thermal capacities leads to longer discharge duration, working as a thermal energy reservoir that supplies heat to the activated carbon bed during the discharge process, and thus, partially compensating for the latent heat of adsorption cooling effects.

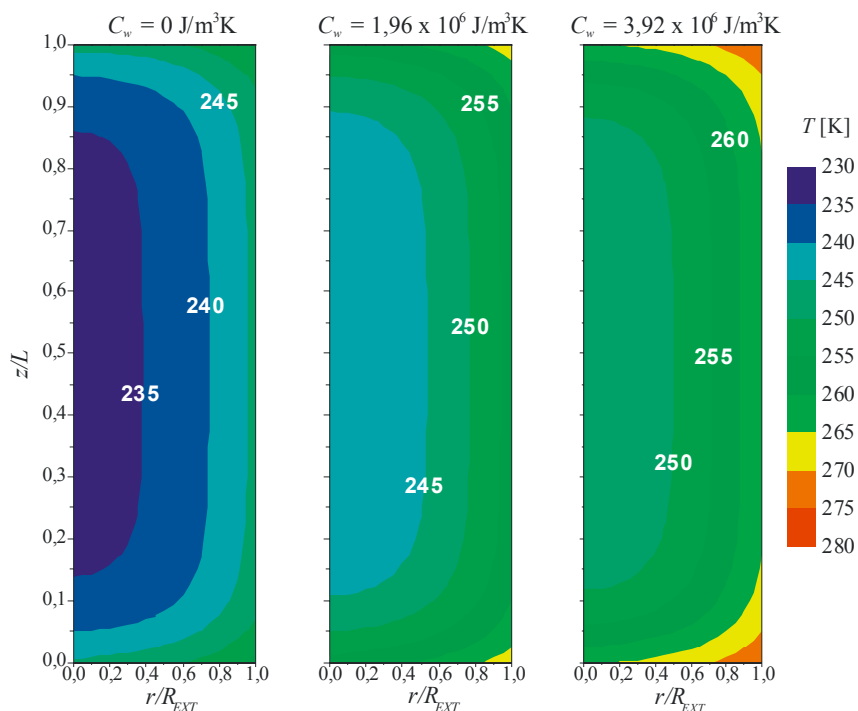


Figure 8: Temperature distribution within the adsorbent bed for $T_\infty = 19\text{ }^\circ\text{C}$ and $\dot{m} = 0,3283\text{ g/s}$ at depletion pressure.

Table 6. Results for the cylinder thermal capacity analysis.

C_w [J/m ³ K]	Discharged Mass [kg]	η [%]	Discharge Time [h]
0	2,116	78,68	1,79
$1,96 \times 10^6$	2,279	84,76	1,93
$3,92 \times 10^6$	2,367	88,02	2,00

5. Conclusion

The intensification of the gas discharge capacity of adsorbed natural gas reservoirs was discussed in this paper. A literature review regarding experimental and theoretical studies performed on the charge and discharge processes of adsorbed natural gas reservoirs was presented, and a two-dimensional transient model for the slow discharge process developed by the authors was used for the discussions.

A simple model for a heat pipe was introduced in the adsorbed natural gas discharge model to investigate the effects of the activated carbon bed thermal control on the discharge duration. The coupled model was able to simulate the reservoir thermal control and an increase in the discharge duration of up to 35 minutes was observed for $\dot{m} = 0,1641$ g/s and a heat source temperature of 300 °C. The advantage of using heat pipes for the thermal control of adsorbed natural gas reservoir is that this kind of device can work in both heat transfer directions, *i.e.*, it can be used to supply heat or to remove heat from the reservoir.

The analysis of the convection heat transfer at the external wall of the adsorbed natural gas cylinder showed that the surrounding temperature plays an important role in the discharge duration. The convection heat transfer should be done in a controlled way to prevent high activated bed temperature gradients, which can lead to high pressures, eliminating the advantages of low pressure reservoirs.

The effective thermal conductivity of the activated carbon structure is also an important parameter as it can smooth the temperature gradients within the adsorbent bed, improving the heat transfer by convection from the cylinder wall, or improving the performance of the thermal control device, leading to an extension of the discharge duration time.

The heat capacity of the cylinder wall can also help on the extension of the discharge duration by acting as a thermal energy reservoir, providing heat to the adsorbent bed, and partially compensating the cooling effects imposed by the latent heat of adsorption.

6. Nomenclature

C_w	Heat capacity of the cylinder wall
c_p	Isobaric heat capacity
h_f	Forced convection heat transfer coefficient
h_w	Heat transfer coefficient at cylinder wall
k_{eff}	Effective thermal conductivity
k_{HP}	Heat pipe effective thermal conductivity
L	Cylinder length
L_{evap}	Heat pipe evaporator length
\dot{m}	Mass flow rate
\mathbf{n}	Normal direction
P	Pressure
P_d	Depletion pressure
q	Adsorbed phase concentration
R	Radius
R_0	Cylinder filling opening radius
R_{ext}	Cylinder external radius
r	Radial coordinate
T	Temperature
T_f	Heat source temperature (heat pipe)

T_∞	Surrounding temperature
t	Time
V	Volume
z	Axial coordinate

Greek Symbols:

ΔH	Latent (isosteric) heat of adsorption
δ_w	Cylinder wall thickness
φ_{eff}	Effective porosity
ρ	Density
η	Performance coefficient

Subscripts:

$()_a$	Adsorbed phase
$()_g$	Gas phase
$()_{HP}$	Heat pipe
$()_s$	Solid phase
$()_w$	Cylinder wall properties
$()_0$	Initial condition

7. Acknowledgement

The authors would like to acknowledge CNPq for funding this research. Luciano G. Lara would like to acknowledge Petrobras S/A – ENGENHARIA/IEABAST/EAB/ENPRO for supporting this work.

8. References

- Bejan, A., 1995. **Convection Heat Transfer**. 2nd Ed., New York, NY: John Wiley & Sons, Inc.
- Biloé, S.; Goetz, V.; and Mauran, S., 2001a. “Dynamic Discharge and Performance of a New Adsorbent for Natural Gas Storage”. In: *AIChE Journal*, Vol. 47, no. 12, pp. 2819-2830.
- Biloé, S.; Goetz, V.; and Mauran, S., 2001b. “Characterization of adsorbent composite blocks for methane storage”. In: *Carbon*, Vol. 39, pp. 1653–1662.
- Biloé, S.; Goetz, V.; and Guillot, A. “Optimal Design of an Activated Carbon for an Adsorbed Natural Gas Storage System”. In: *Carbon*, 2002, Vol. 40, pp. 1295-1308.
- Brady, T. A.; Rostam-Abadi, M.; and Rood, M. J., 1996. “Applications for Activated Carbons from Waste Tires: Natural Gas Storage and Air Pollution Control”. In: *Gas Separation and Purification*, Vol. 10, no. 10, pp. 97-102.
- Burchell, T. and Rogers, M., 2000. “Low Pressure Storage of Natural Gas for Vehicular Applications”. SAE Tech. Paper Series no. 2000-01-2205, In: Government/Industry Meeting, Washington, D.C.
- Chang, K. J. and Talu, O., 1996. “Behavior and Performance of Adsorptive Natural Gas Storage Cylinders During Discharge”. In: *Applied Thermal Engineering*, Vol. 16, no. 5, pp. 359-374.
- Faghri, A., 1995. **Heat Pipe Science and Technology**. Taylor & Francis, Washington DC.
- Gregg, S. J. and Sing, K. S. W., 1982. **Adsorption, Surface Area and Porosity**. 2nd ed., London: Academic Press, Inc.
- Inomata, K.; Kanazawa, K.; Urabe, Y.; Hosono, H. and Araki, T., 2002. “Natural gas storage in activated carbon pellets without a binder”. In: *Carbon*, Vol. 40, pp. 87-93.
- Lara, L. G., 2005. **Theoretical Analysis of the Discharge Process of Adsorbed Natural Gas Reservoirs** (*original in Portuguese*). M. Sc. thesis, Mech. Eng. Programme, Fed. Univ. of Rio de Janeiro, Brazil.
- Lara, L. G.; Couto, P.; Sophya, D. M. A.; and Cotta, R. M., 2006. “Thermal Control of Adsorbed Natural Gas Reservoirs During Discharge Dynamic Conditions”. 13th International Heat Transfer Conference, Sydney, Australia, 14th to 18th Aug. Proceedings (CD-ROM).
- Litzke, W. L. and Wegrzyn, J., 2001. “Natural Gas as a Future Fuel for Heavy-Duty Vehicles”. SAE Tech. Paper Series n°2001-01-2067, In: Government/Industry Meeting, Washington, D.C.
- MacDonald, J. A. F. and Quinn, D. F., 1998. “Carbon Adsorbents for Natural Gas Storage”. In: *Fuel*, Vol. 77, no. 1, pp. 61-64.
- Moran, M. J. and Shapiro, H. N., 2000. **Fundamentals of Engineering Thermodynamics**. 4th Edition, New York, NY: John Wiley & Sons, Inc.
- Mota, J. P. B.; Rodrigues, A. E.; Saadatian, E.; and Tondeur, D., 1997. “Dynamics of Natural Gas Adsorption Storage Systems Employing Activated Carbon”. In: *Carbon*, V.35, n°9, pp.1259-1270.
- Mota, J. P. B.; Esteves, I. A. A. C.; and Rostam-Abadi, M., 2004. “Dynamic modelling of an adsorption storage tank using a hybrid approach combining computational fluid dynamics and process simulation”, In: *Computers and Chemical Engineering*, n° 28, pp. 2421–2431.
- Peterson, G. P., 1991. **An Introduction to Heat Pipes – Modeling, Testing and Applications**. 1st ed., John Wiley and Sons, Inc., New York, NY.
- Tien, C., 1994. **Adsorption Calculations and Modeling**. 1st Edition, Newton, MA: Butterworth-Heinemann series in chemical engineering.
- Vasiliev, L. L.; Kanonchik, L. E.; Mishkinis, D. A.; and Rabetsky, M. I., 2000a. “Adsorbed Natural Gas Storage and Transportation Vessels”. In: *Int. J. of Thermal Sciences*, n° 39, pp. 1047-1055.
- Vasiliev, L. L.; Kanonchik, L. E.; Mishkinis, D. A.; and Rabetsky, M. I., 2000b. “A New Method of Methane Storage and Transportation”. In: IV Minsk International Seminar on Heat Pipes, Heat Pumps and Refrigerator, Minsk, Belarus, September 4-7, Proceed-ings, pp. 218-228.

9. Copyright Notice

The author is the only responsible for the printed material included in his paper.